# Mass Spectrometric Investigation of the Pyrolysis of Boranes. IV. Diborane[1]

**Anthony B. Baylis, George A. Pressley, Jr., and Fred E. Stafford**

*Contribution from the Department of Chemistry and The Materials Research Center, Northwestern University, Evanston, Illinois 60201.* *Received November 13, 1965*

**Abstract:** A mass spectrometer was used to observe directly the contents of a flow reactor in which diborane at low pressure was being pyrolyzed. Temperature, flow time, surfaces, and gas pressures were varied. Borane, $BH_3$, was clearly identified and its mass spectrum measured. A novel method, involving the difference in reactivities of monomer and dimer, was used to distinguish between $BH_x^+$ ions due to neutral borane and to fragmentation of diborane. The formation of higher boranes was followed. Secondary process ions also were measured.

Kinetic studies of the $B_2H_6$ pyrolysis reaction implicate $BH_3$ as a reaction intermediate.[2,3] The energy required to dissociate diborane into two boranes has been calculated from electronegativities,[4] thermochemical extrapolation,[5,6] kinetic data for the decomposition of $BH_3CO$,[7-9] and electron-impact studies.[9] The values obtained range from 24 to 38 kcal/mole.

An independent mass spectrometric study of diborane pyrolysis by the present authors[10] yielded data from which was calculated the sum of $D(BH_3BH_3)$ plus any kinetic barrier to dissociation equal to 55 ± 8 kcal/mole. A monoborane species, believed to be $BH_3$, was observed at temperatures above 650°K.

Apart from the interest in the value of $D(BH_3BH_3)$, considerable attention has been given the mechanism by which diborane reacts to produce the higher members of the boron hydride series. The literature available has been reviewed and summarized.[2,3] In part, there is

$$B_2H_6 \rightleftharpoons 2BH_3 \quad (1)$$

$$BH_3 + B_2H_6 \rightleftharpoons B_3H_9 \rightleftharpoons B_3H_7 + H_2 \quad (2, 3)$$

$$B_3H_7 + B_2H_6 \rightleftharpoons B_4H_{10} \text{ (or } B_4H_8 + H_2) + BH_3 \quad (4)$$

$$B_4H_{10} + BH_3 \rightleftharpoons B_5H_{11} + H_2 \quad (5)$$

$$B_4H_{10} + B_2H_6 \longrightarrow B_5H_{11} + BH_3 + H_2 \quad (6)$$

where reactions 3 and 4 or 4 and 5 may be combined into single steps. In the latter case, pentaborane-11 and not tetraborane would be the first stable intermediate formed.

Also important is the identity of the $B_2H_6$ decomposition product in (1). The results of Fehlner and Koski[8,9] indicate that both $BH_3$ and $BH_2$ may be formed.

Thermochemical predictions[11] show that at *ca.* 2000°K, where $BH_3$ would be formed in equilibrium with B and $H_2$, $BH_2$ also may be abundant. If both species are present, then their mass spectra taken in such a study would overlap and an accurate assignment would be difficult.

The present paper reports on experiments designed to resolve questions about the identity of the monoborane species formed and the contribution of any kinetic barrier to the dissociation energy calculated from our previous mass spectrometric studies.[10] Such tests involve varying the flow time of $B_2H_6$ through the reaction cell, changing surface and surface area, and offering the $B_2H_6$ the opportunity to undergo increasing numbers of both surface and gas-phase collisions with itself and added foreign gases. The mass spectrum of $BH_3$, the spectra of ions produced by various pressure dependent secondary processes, and observation of the polymerization to form higher boranes also are reported.

## Experimental Section

Natural isotope $B_2H_6$ (80% $B^{11}$, 20% $B^{10}$) was prepared by reaction of $KBH_4$ with $H_2SO_4$ and purified prior to use by trap-to-trap distillation at −160.5°. $^{10}B_2H_6$ (96% $^{10}B$) was prepared by the $LiAlH_4$ reduction of $^{10}BF_3 \cdot Et_2O$.

To obtain a sufficiently low pressure of $B_2H_6$ for the pyrolysis experiments, the sample reservoir was maintained at −196° (liquid $N_2$), at which temperature the pressure of diborane is calculated to be $4.4 \times 10^{-7}$ atm,[12] or at the temperature of an isopentane slush.

Argon (99.99%) and helium (oil free, ~100% pure), taken directly from cylinders, were bubbled through a sodium–potassium alloy prior to use. The pressure of the He or Ar entering the Knudsen cell was controlled by incorporating capillaries of varying and accurately measured conductances into the gas entry system. A knowledge of the He or Ar pressure on the high-pressure side of the capillary thus enables one to calculate the resulting pressure in the Knudsen cell.

In all cases the samples were admitted to the mass spectrometer[13,14] through a $^9/_{32}$-in. i.d. stainless steel tube (T, Figure 1), approximately 1 ft long. Affixed to the end of the tube was the reaction cell (A, Figure 1). This is of stainless steel, $^3/_4$-in. i.d., 1 in. high and equipped with three baffles to aid the gas molecules in coming to equilibrium. Such an arrangement offers minimum opportunity for the sample to decompose in the inlet system.

The flow time of the molecules through the cell is varied by changing the size of the knife-edged orifice in the cell lid. Orifices of $1.43 \times 10^{-1}$, $9.2 \times 10^{-3}$, and $1.16 \times 10^{-3}$ cm$^2$ were used, giving calculated flow times through the reactor of 2.6, 40, and 315 msec, respectively.

(1) Supported by the U. S. Atomic Energy Commission, Document COO-1147-6, and by the Advanced Research Projects Agency through the Northwestern University Materials Research Center.

(2) W. N. Lipscomb, "Boron Hydrides," W. A. Benjamin, Inc., New York, N. Y., 1963.

(3) R. M. Adams in "Boron, Metallo-Boron Compounds and Boranes," Interscience Publishers, New York, N. Y., 1964, Chapter 7.

(4) L. Pauling, "The Nature of the Chemical Bond," Cornell University Press, Ithaca, N. Y., 1960.

(5) R. E. McCoy and S. H. Bauer, *J. Am. Chem. Soc.*, 78, 2061 (1956); *cf.* also ref 6.

(6) S. G. Shore, C. W. Hickam, Jr., and D. Cowles, *ibid.*, 87, 2755 (1965).

(7) M. E. Garabedian and S. W. Benson, *ibid.*, 86, 176 (1964).

(8) T. P. Fehlner and W. S. Koski, *ibid.*, 86, 2733 (1964).

(9) T. P. Fehlner and W. S. Koski, *ibid.*, 87, 409 (1965).

(10) E. J. Sinke, G. A. Pressley, Jr., A. B. Baylis, and F. E. Stafford, *J. Chem. Phys.*, 41, 2207 (1964).

(11) Joint Army-Navy-Air Force Thermochemical Tables, The Dow Chemical Co., Midland, Mich.

(12) B. S. Yaffe, "Diborane," Callery Chemical Co., Callery, Pa., 1962.

(13) The mass spectrometer was built by Nuclide Analysis Associates, Model 12-60-HT, according to the design of ref 14.

(14) W. A. Chupka and M. G. Inghram, *J. Phys. Chem.*, 59, 100 (1955); M. G. Inghram and J. Drowart in "High Temperature Technology," McGraw-Hill Book Co., Inc., New York, N. Y., 1960, p 219.

In the case of the 1.16 and 9.2 × $10^{-3}$ $cm^2$ orifices, the main pressure drop occurred at the orifice, giving a well-defined pressure in the reaction cell. This pressure was calculated[15] from the conductances of the tubes and metering valve of the inlet system and the known vapor pressures of diborane. For a given constant temperature bath, it could be varied also by closing the metering valve.

The orifice acts as the source of a molecular beam that is defined by the movable slit D and a series of four increasingly narrow slits that precede the ion source ionizing electron beam. The distance from the orifice to the electron beam is about 6 cm.

The vacuum chamber housing the ion source is water cooled so that changes in reactor temperature have minimal effect upon the source characteristics.

The movable beam defining slit D (0.040 in.) and the slit (0.020 in.) just before the ionizing electron beam in the source are of such dimensions that they define the line that the molecules must travel in order to be ionized and eventually detected. As the shutter D is moved from right to left by the micrometer screw M, neutrals originating on the radiation screens C, the reactor, the reactor orifice, and again the reactor and the screens are "seen" by the ion source. Residual or background gases are not at all affected by movement of the shutter (except where the slit is closed off by the support plate).

A plot of ion intensity *vs.* shutter position produces a shutter profile,[14] the shape of which indicates whether the observed species originate directly from the crucible orifice or are produced on the crucible lid, heating elements, heat shields, etc. Molecules so identified as originating directly from the orifice pass through the ion source without having the chance to be pyrolyzed (or, in the case of isotopically labeled materials, scrambled) on the hot source surfaces, hence the importance of zero source contact mass spectra.

The ratio of ion intensity due to species emanating directly from the orifice (molecular beam species) to the total ion intensity at a given mass peak is called the "per cent shutter effect."

Because of the importance of the shutter profile and the zero source contact mass spectra, the apparatus was designed for severe collimation of the molecular beam, such that this beam includes only $10^{-2}$% of the material effusing from the orifice. The remainder must be pumped away rapidly to prevent the buildup of a high background pressure which would swamp the molecular beam signal. This necessitates the use of an efficient differential pumping system, the details of which are significant for the success of the experiment.

The only connection between the ion source and reaction cell chambers is the slit D. The chamber housing the cell is pumped with a 6-in. mercury diffusion pump combined with a titanium vaporization getter pump to give an estimated total pumping speed for reactive gases of about 400–500 l./sec *in* the chamber. The pressure differential across the 1-mm diameter cell orifice is thus on the order of 4000:1.

About 20 l./sec pumping speed is obtained in the ion source chamber with the consequent factor of 10 to 20 pressure differential across slit D. With only the mercury pumps running, the molecular beam gives rise to *ca.* 15% of the observed diborane ion intensities (*i.e.*, 15% shutter effect). When the titanium vaporization pump also is running, only the background $B_2H_6$ is reduced and the shutter effect increases to 25–30%. This high-speed pumping system, therefore, is necessary for the experiments to be described.

In the case of species pumped rapidly by the vacuum chamber walls, such as the reaction intermediate $BH_3$, the shutter effect approaches 100%. Therefore, this is an important diagnostic for these reactive intermediates.

Normally, ions were formed with 70-ev electrons and were accelerated through 4000 ev into the 60° magnetic sector, 12-in. radius of curvature, mass analyzer. The resolved ions were detected with either a 50% transmission grid (classical collector) or accelerated through an additional 3250 ev onto the dynode of a 16-stage Be-Cu secondary electron multiplier. Under normal operating conditions, with the 1-mm reactor orifice, the detectability limit was $10^{-10}$ atm partial pressure in the reaction cell or $10^{-14.5}$ atm in the ion source chamber.

Because of this high sensitivity, even with a base pressure of $10^{-11}$ atm, background peaks could be counted at almost every mass up to *m/e* 200 and were quite large at a number of peaks of interest in this study. However, with narrowed analyzer exit slit, the mass analyzer could resolve the boron hydrides from the ubiquitous hydrocarbon background. This permitted detection even of very small boron hydride ion intensities as well as unambiguous identification of ions through the positive mass defect of boron. Spectra demonstrating this mass resolution are shown elsewhere.[16] Under standard operating conditions, the exit slit was opened so that intensities due to all the isotopic boron hydride ions occurring at a given mass number were measured together.

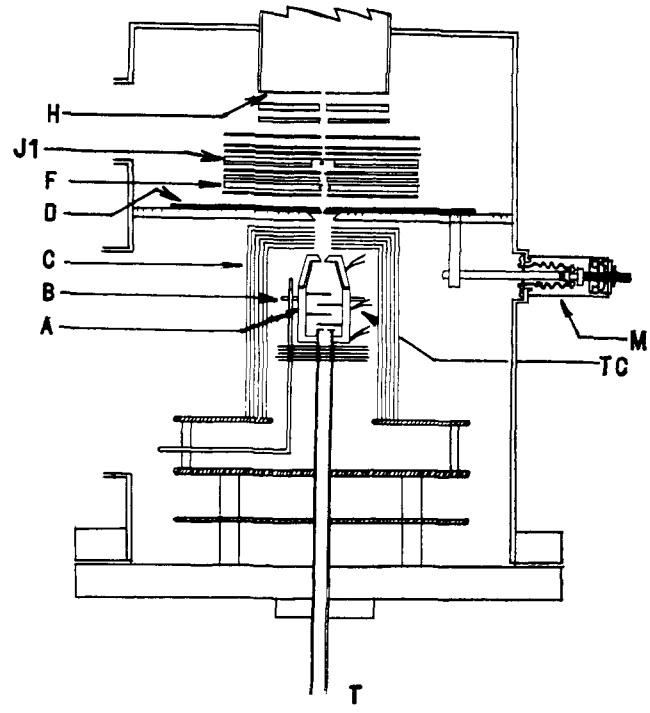


Figure 1. Furnace and ion source region of special mass spectrometer: A, reaction cell; B, heating filament; C, radiation screens; D, movable molecular beam defining slit; F, one of the additional four beam defining slits (the narrowest of these, 0.020 in., is just below the plate labeled J1); J1, the "ion box." The ionizing electron beam is shown as a circle at the center of this plate; H, entrance slit to mass analyzer; M, micrometer assembly for D; TC, one of the three thermocouples; T, sample inlet tube. The furnace chamber is pumped by a 6-in. mercury diffusion pump; the source and analyzer regions are pumped by 2-in. pumps.

## Results and Discussion

Ions and their neutral progenitors were identified using mass spectrum or isotope ratios, mass defect, appearance potentials, dependence on temperature, dependence on inlet valve setting, and shutter profile.

Table I. Zero Source Contact Mass Spectra of (A) $^{10}B_2H_6$ (96% $^{10}B$) and (B) Normal Isotopic Composition $B_2H_6$ with 70-ev Ionizing Electrons, 4-kev Ion Acceleration, and Multiplier Detection of 7250-ev Ions

| A | | B | |
|---|---|---|---|
| *m/e* | Rel intensity | *m/e* | Rel intensity |
| 26 | 6.8 | 27 | 100 |
| 25 | 100 | 26 | 95.5 |
| 24 | 43.7 | 25 | 44.7 |
| 23 | 23.3 | 24 | 67.5 |
| 22 | 52.3 | 23 | 33 |
| 21 | 4.4 | 22 | 6.5 |
| 20 | 1.5 | 21 | 1.5 |
| 13 | 0.33 | 13 | 10.4 |
| 12 | 7.2 | 12 | 6.1 |
| 11 | 3.0 | 11 | 11.7 |
| 10 | 6.6 | 10 | 3.0 |

(15) S. Dushman, "Scientific Foundations of Vacuum Technique," 2nd ed, revised by J. M. Lafferty, John Wiley and Sons, Inc., New York, N. Y., 1962.

(16) A. D. Norman, R. Schaeffer, A. B. Baylis, G. A. Pressley, Jr., and F. E. Stafford, *J. Am. Chem. Soc.*, **88**, 2151 (1966).

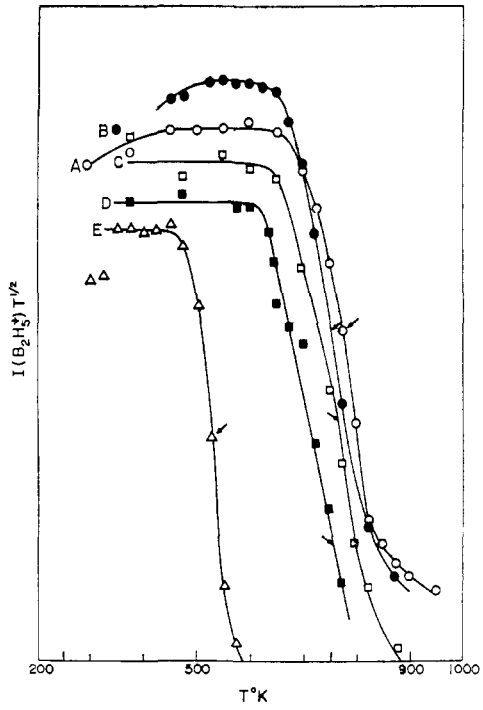


Figure 2. Mass flow of diborane $[I(B_2H_5^+)T^{1/2}]$ *vs.* $T$°K. In all cases a $9.2 \times 10^{-3}$ cm² orifice (nominal 40-msec flow time) was used. For A–D a liquid nitrogen bath was used on the reservoir. Curve A: $B_2H_6$ alone; cell pressure $5 \times 10^{-8}$ atm with about $10^1$ "self"-collisions and $10^3$ wall collisions. Curve B: reaction cell packed with quartz wool; the measured ion intensity was reduced 30% from that of (A); the scales have been changed, however, so that the two overlap. Curves C and D: with $8.3 \times 10^{-5}$ and $1.9 \times 10^{-3}$ atm of argon; the diborane ion intensities have been reduced by factors of 3 or 4 owing to diffusion limitations; the Ar–$B_2H_6$ collisions are estimated at $3.6 \times 10^4$ and $8 \times 10^4$, respectively. Curve E: diborane at $5 \times 10^{-6}$ atm (liquid oxygen bath).

For comparative purposes the curves have been scaled and translated vertically so as to fit on the same diagram. As indicated the diborane intensity does not necessarily fall to zero as the bottom of the figure is reached. The temperature at which the mass flow has been reduced by 50% is indicated on each curve by an arrow, specifically 775, 760, 765, 755, and 525°K, respectively.

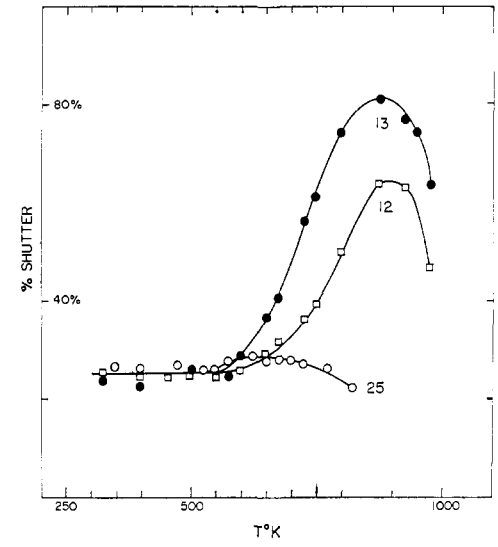


Figure 3. Fraction of observed ion intensity due to molecular beam species (% shutter) *vs.* $T$°K for *m/e* 25 ($^{10}B_2H_5^+$), *m/e* 12 ($^{10}BH_2^+$), and *m/e* 13 ($BH_3^+$); initial $P(B_2H_6) = 5 \times 10^{-8}$ atm; cell orifice $= 9.2 \times 10^{-3}$ cm² (40-msec flow time).

Only the shutterable portion of each peak is considered. Therefore these mass spectra are for zero ion source contact.

The mass spectra of $^{10}B_2H_6$ (96% $^{10}B$) and $^{n}B_2H_6$ are given in Table I. As long as there was no evidence of diborane decomposition, these spectra were sensibly independent of reaction cell temperature. Even with extensive diborane decomposition, the intensities of the $B_2H_x^+$ peaks relative to one another remained the same. Consequently, the major peak, *m/e* 27 for $^{n}B_2H_6$ (or *m/e* 25 for $^{10}B_2H_6$) was henceforth used as a measure of total diborane ion intensity.

Measurements were made at each temperature only when the crucible temperature was constant to ±1°. At 873°K, nearly the highest temperature used, the thermocouples attached to the bottom and middle of the crucible registered identical readings; that attached to the crucible cap read 6° higher (1° at 573°K).

Under molecular flow conditions the mass flow of diborane into the reaction cell is controlled predominantly by the conductance of the conduits that were maintained at nearly constant temperatures. As the crucible temperature is raised, molecular beam velocity increases and the number density of molecules in the volume intersected by the ionizing electron beam should decrease, causing a consequent decrease in measured ion current. Therefore, as long as no decomposition occurs, a plot of $I(25^+)T^{1/2}$ *vs.* $T$ should vary nearly linearly. This is shown in Figure 2 for a variety of experimental conditions which are specified in the figure caption.

**Identification of Monoborane.** As indicated previously,[10] ion intensities due to monoborane(s) were observed at temperatures corresponding to the knees of the curves in Figure 2. To identify the monoborane species, $^{10}B_2H_6$ (96% $^{10}B$) was used. This offers the advantages of avoiding troublesome background at *m/e* 14, providing simpler mass spectra and giving a larger mass defect with respect to the ubiquitous hydrocarbon background.

With $P(B_2H_6) = 5 \times 10^{-8}$ atm in the reaction cell and nominal 40-msec flow time through the reactor, the ion peaks due to $^{10}B_2H_5^+$, $^{10}BH_3^+$, and $^{10}BH_2^+$ were monitored as a function of cell temperature. From 300 to 650°K, the shutter effect on all three peaks was approximately 25%. (The titanium getter pump was used throughout the run.)

With increasing temperature above 650°K, the shutter effect on *m/e* 25 remains constant between 22 and 28%, while those on *m/e* 12 and *m/e* 13 reach as high as 64 and 81%, respectively (Figure 3). Simultaneously there is a sharp decrease in absolute intensity of *m/e* 25 but an increase for *m/e* 12 and *m/e* 13 (Figure 4). The maximum intensity of the *m/e* 13 peak occurs at about 800°K when approximately 80% of the diborane has been decomposed. At this temperature $I(25^+)/I(13^+) = 10$ and $I(25^+)/I(12^+) = 2.82$ compared to values of 300 and 14, respectively, from parent $^{10}B_2H_6$.

The smaller fractional increase in intensity and shutter effect for *m/e* 12 relative to *m/e* 13 is ascribed to the larger contribution that the fragmentation of $B_2H_6$ makes at this mass. This is a good demonstration of the fact that $B_2H_6$ forms a stable background whereas the monoborane does not. It shows also the impor-

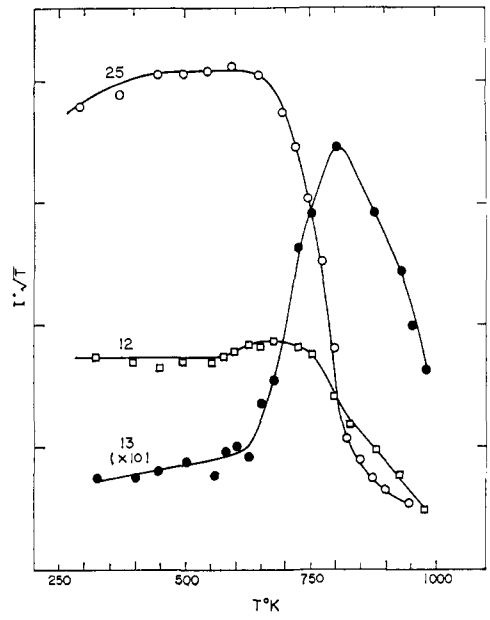


Figure 4. Mass flow ($I^+\sqrt{T}$) as a function of temperature, for $I(25^+)\sqrt{T}$, $I(12^+)\sqrt{T}$, and $I(13^+)\sqrt{T}$; same run as Figures 3 and 5.

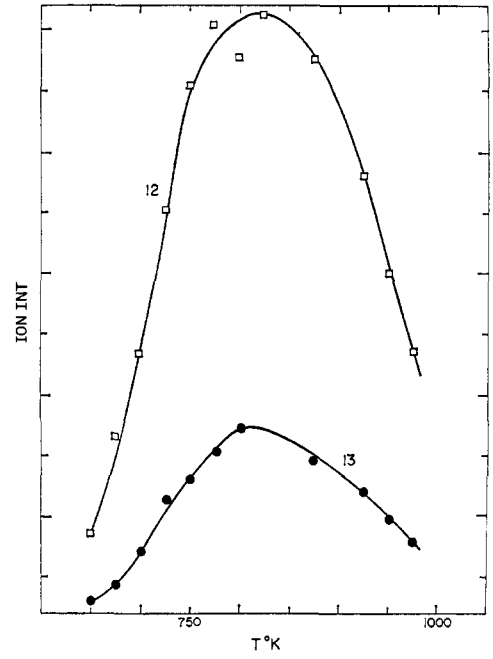


Figure 5. Intensity (mv) of $I(^{10}BH_2^+)$ and $I(^{10}BH_3^+)$ (mass peaks 12 and 13) as a function of temperature. The contribution that the fragmentation of $^{10}B_2H_6$ makes at these masses has been subtracted out. These data were taken from the same runs as for Figures 3 and 4.

tance of the shutter for these studies, and specifically its power as a diagnostic for unstable intermediates; it has precluded that the increase of intensities of the lower mass peaks be due to a temperature-induced change in fragmentation pattern.

No significant change in the mass spectrum of $^{10}B_2H_6$ was observed from 300 to 650°K. The large increase in absolute intensity at *m/e* 13 and 12 must be due to the ionization and fragmentation of at least one new species. Since increase in intensity occurred only at masses 10 through 13 (and not 20 through 26 or higher), the new species is taken to contain only one boron atom.

The contributions that the fragmentation of $^{10}B_2H_6$ makes to masses 13 and 12 were subtracted out and the resulting $I(13^+)$ and $I(12^+)$ plotted as a funtion of temperature (Figure 5). From 650 to 925°K the ratio $[I(12^+)/I(13^+)]$ remains constant at 3.2 ± 0.2, indicating the presence of only one monoborane species.

Monoborane was observed also for a 2.6-msec flow time. In this case $I(12^+)/I(13^+)$ was 3.0 ± 0.3 between 700 and 850°K. Similar results obtained at $5 \times 10^{-6}$ atm (Figure 2c) give, in addition to higher boranes to be discussed below, $I(12^+)/I(13^+) = 2.96 \pm 0.15$.

Although the molecular beam intensities of $^{10}BH_3^+$ and $^{10}BH_2^+$ from the monoborane(s) were too low for accurate determination of appearance potentials, rough measurements indicate $AP(BH_2^+) \geq AP(BH_3^+)$. Both were in the range 11.0 to 12.0 ev.

In similar fashion, the relative intensities for $B^+$ and $BH^+$ were determined over the same temperature range. The high appearance potential for $BH_2^+$, coupled with the constancy of the monoborane mass spectrum over a 275° temperature range, indicates that only $BH_3$ was observed. Its complete mass spectrum is presented in Table II where it is also compared to group III halides believed to have a similar configuration.

Although no evidence for $BH_2$ was observed in the present work, this alone does not prove reactions 1–6 to be the homogeneous pyrolysis mechanism rather than one involving $BH_2$ as proposed by Fehlner;[17] $BH_2$ could in the present case be preferentially destroyed by wall reactions. When the products of the decomposition of $B_2H_6$ in a shock tube were examined[18] using a time-of-flight mass spectrometer, the ratio $I(13^+)/I(14^+)$ was 10 or 20 to 1. The ratio computed from the present data is 3:1. This suggests, differences in mass analyzer notwithstanding, that $BH_2$ may be present in quantity and may be responsible for shock tube induced polymerization of $B_2H_6$.

**Table II.** Mass Spectra of $BX_3$[a]

| | X | | | | |
|---|---|---|---|---|---|
| | H[b] | F[c] | Cl[c,d] | Br[d] | I[d] |
| $BX_3^+$ | 31 | 3 | 36 | 37 | ... |
| $BX_2^+$ | 100 | 100 | 100 | 100 | 100 |
| $BX^+$ | 16 | 1 | 8 | 49 | 22 |
| $B^+$ | 8 | 3 | 3 | 0.5 | 9 |

[a] The mass spectra of $YCl_3$ and $AlCl_3$ also are very similar: J. D. McKinley, *J. Chem. Phys.*, **42**, 2245 (1965); R. F. Porter and E. E. Zeller, *ibid.*, **33**, 858 (1960). [b] Present work. [c] O. Osberghaus, *Z. Physik*, **128**, 366 (1950). [d] W. S. Koski, J. J. Kaufman, and C. F. Pachuki, *J. Am. Chem. Soc.*, **81**, 1326 (1959).

**Higher Boranes and Secondary Process Ions.** At diborane reactor pressures above $10^{-4}$ atm, ions containing three or four, but not five, boron atoms were observed with crucible temperatures as low as 10°. Above 150°, ions containing five boron atoms appeared; their intensity increased with increasing temperature. Figure 6 shows the relative intensities of the $B_3$ and the $B_4$ ions. Table III shows the partial mass spectrum

(17) T. P. Fehlner, *J. Am. Chem. Soc.*, 87, 4200 (1965).
(18) R. W. Diesen, Dow Chemical Co., private communication.

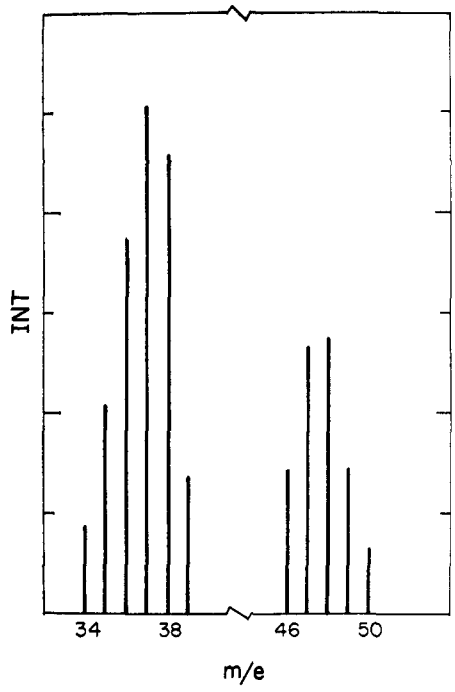


Figure 6. Relative intensities of secondary process ions produced in the ion source chamber during high-pressure diborane run ($^{n}B_2H_6$).

of the $B_5$ ions compared to literature spectra of $B_5H_9$ and $B_5H_{11}$;[19] it is most similar to that of $B_5H_9$.

Table III. Mass Spectrum of the Pentaborane Observed during the *in situ* Pyrolysis of $^{n}B_2H_6$

| *m/e* | $B_5H_{11}$[a] | Present work | $B_5H_9$[a] |
|---|---|---|---|
| 64 | 18 | 52 | 52 |
| 63 | 27 | 58 | 62 |
| 62 | 84 | 80 | 80 |
| 61 | 99 | 53 | 70 |
| 60 | 100 | 100 | 99 |
| 59 | 97 | 100 | 100 |
| 58 | 57 | 50 | 66 |

[a] Reference 19.

Data from this and other runs indicate that the intensity of $B_3$ and $B_4$ ions observed at low temperatures and high pressures depend roughly on the square of diborane ion intensity which in turn is proportional to the background pressure in the ion source. The intensity of these heavier ions is relatively insensitive to temperature, and the $B_4$ to $B_3$ ion intensity ratio remains sensibly constant. Accordingly, they are assigned to secondary processes in the ion source involving reaction of $B_2H_x^+$ with neutral diborane. The mass spectrum of Figure 6 is identical with one reported[20] by us previously for $B_4H_8$. This was due to a time-dependent increase in ambient diborane pressure which paralleled the temperature increase. Identification of $B_4H_8$ produced during the pyrolysis of $B_4H_{10}$ has been reported elsewhere.[21]

(19) I. Shapiro, C. O. Wilson, J. F. Ditter, and W. J. Lehmann, Advances in Chemistry Series, No. 32, American Chemical Society, Washington, D. C., 1961, p 127.

(20) A. B. Baylis, G. A. Pressley, Jr., and F. E. Stafford, *J. Am. Chem. Soc.*, **86**, 5358 (1964).

(21) A. B. Baylis, G. A. Pressley, Jr., M. E. Gordon, and F. E. Stafford, *ibid.*, **88**, 929 (1966).

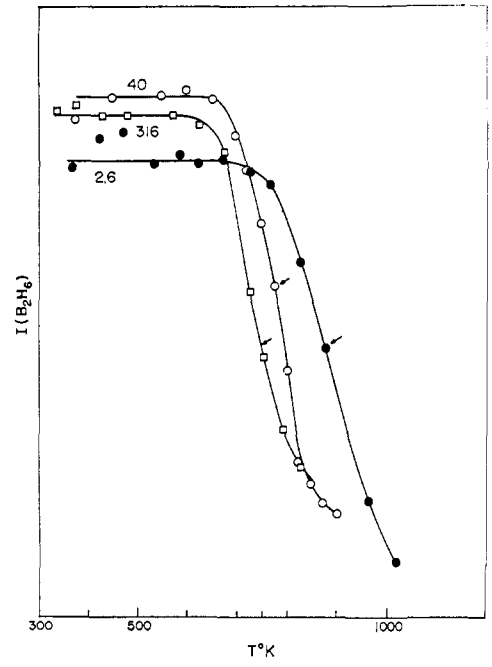


Figure 7. Mass flow of diborane as a function of orifice size and temperature. Diborane reservoir maintained in liquid nitrogen for each case. Curve a: orifice area = $1.43 \times 10^{-1}$ cm²; cell "pressure" = $4.4 \times 10^{-9}$ atm; nominal flow time of $B_2H_6$ in cell, 2.6 msec; $BH_3$ observed above 700°K. Curve b: orifice area = $9.2 \times 10^{-3}$ cm²; cell pressure = $5.2 \times 10^{-8}$ atm; nominal flow time of $B_2H_6$ in cell, 40 msec; $BH_3$ observed above 650°K. Curve c: orifice area = $1.16 \times 10^{-3}$ cm²; cell pressure = $1.6 \times 10^{-7}$ atm; nominal flow time, 315 msec. Neither $BH_3$ nor higher polymers observed.

As in Figure 3 the curves have been adjusted to fit on the same scale. The temperature at which the diborane mass flow is reduced by 50% is arrowed in each case. These are 875, 775, and 750°K for 2.6, 40, and 315 msec, respectively.

**Dissociation of $B_2H_6$.** In none of the runs was the ion intensity of $BH_3$ greater than 2 or 3% of that due to the $B_2H_6$ entering the reactor. Hydrogen effusing from the reactor was observed and a dark, metal-like deposit was formed on the reactor surfaces and on the quartz wool to be discussed below. Consequently the favored path of reaction under these conditions is not the desired homolytic dissociation.

Figure 2E shows that diborane could effectively lower the temperature at which decomposition was observed. This cannot be attributed simply to the effectiveness of diborane as an energy transfer agent because higher boranes were observed, showing that an additional reaction path may have been opened.

To avoid this difficulty, the reactor was packed with quartz wool. The results are shown in Figure 2B. The flow of diborane through the reactor was reduced by 30% indicating the effectiveness of the packing in producing additional collisions by which the diborane might come to equilibrium. The extent of reaction as a function of temperature is seen to coincide almost exactly with that for no packing.

Next the pyrolysis experiments were repeated in the presence of various pressures of argon (Figure 2C, D). For the highest argon pressure, which corresponds to partial transition to viscous flow, the decomposition temperatures appear to be shifted down by as much as 50° (Figure 2D).

Finally the reactor orifice size, and hence the flow time through the reactor, was varied. Figure 7 shows that there seems to be a well-defined systematic effect (arrows indicate point of 50% decomposition).

For pressures of $5 \times 10^{-6}$ atm and below, the mean free path is approximately equal to or greater than the reactor dimensions. Consequently, the composition must become nearly uniform throughout the cell. This is a condition defining a "stirred flow reactor." [22] Reaction time is assumed to be determined only by the cell orifice; any products formed, however, can leave either by the orifice or by the inlet. The formula for a first-order reaction in a stirred flow reactor is

$$k = F_B V_R/(I^0 - I)/I \qquad (7)$$

where $k$ is the rate constant; $F_B$ is the flow rate through the orifice; $V_R$ is the effective reactor volume, taken in all cases to be the measured volume; $I$ and $I^0$ are the pressures of diborane with and without reaction. $I$ was taken equal to the measured ion intensity; since intensity ratios are used, other factors cancel. $I^0$ was obtained arbitrarily from a horizontal extrapolation of the low-temperature ion intensities.

Equations based on three other sets of assumptions are available[23] for reduction of the data. These are for the stirred flow reactor with volume effect, and for viscous (plug) flow reactors with and without volume effect. The "volume effect" takes into account that the contact time is systematically shortened if the volume of the products is greater than that of the reactants. It applies neither where the mean free path is large nor where the reactants are diluted by a large quantity of inert gas. Similarly, plug flow does not obtain if the mean free path is large compared to the reactor dimensions.

The Arrhenius plot of the rate constants obtained using eq 7 is shown in Figure 8. The data for the three reactor flow times fall on three lines which fall close enough together to be explained by a small error in the effective contact time, $V_R/F_B$. Another possibility is that the diborane pressure, which is known to affect markedly the rate at higher pressures and which varies systematically with the reactor orifice size, may be playing a small role. Rate constants calculated assuming the reaction second order with respect to diborane are not self-consistent.

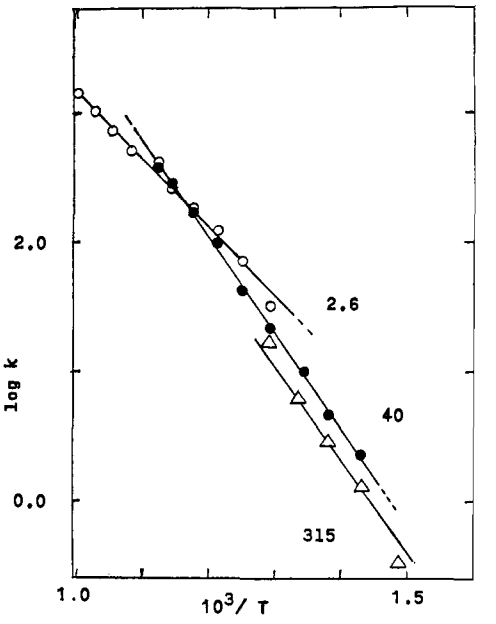


Figure 8. Arrhenius plot, log $K$ *vs.* $10^3/T$ for reactors with orifices corresponding to 2.6-, 40-, and 315-msec flow times.

For the reactor with the 2.6-msec flow time, the conductance of the exit orifice is approximately equal to that of the remainder of the reactor. Consequently, pressure in this case is a poorly defined quantity. The points on the Arrhenius plot for this reactor fall on a line with slope smaller than those for the other two reactors.

To convert these data to a dissociation energy for diborane, it is necessary to know the reaction mechanism. The data presented show that the mechanism is not well defined under these conditions, and that our previous value of 55 kcal/mole is not substantiated. While further work might make this approach more fruitful, it is more attractive at this time to attempt to determine the dissociation energy by direct measurement of the high-temperature equilibrium between hydrogen and solid boron.

(22) A. A. Frost and R. G. Pearson, "Kinetics and Mechanism," 2nd ed, John Wiley and Sons, Inc., New York, N. Y., 1961.
(23) G. M. Harris, *J. Phys. Colloid Chem.*, **51**, 505 (1947).